

RESEARCH ARTICLE

Concurrent Mutations in *ATM* and Genes Associated with Common γ Chain Signaling in Peripheral T Cell Lymphoma

Haley M. Simpson^{1,2}, Rashid Z. Khan^{1,2}, Chang Song^{1,2}, Deva Sharma^{1,2}, Kavitha Sadashivaiah^{1,2}, Aki Furusawa^{1,2}, Xinyue Liu³, Sushma Nagaraj³, Naomi Sengamalay³, Lisa Sadzewicz³, Luke J. Tallon³, Qing C. Chen⁴, Ferenc Livak^{1,5}, Aaron P. Rapoport¹, Amy Kimball¹, Arnob Banerjee^{1,2*}

1 Program in Oncology, Greenebaum Cancer Center, Department of Medicine, University of Maryland School of Medicine, Baltimore, MD, United States of America, **2** Center for Stem Cell Research and Regenerative Medicine, University of Maryland School of Medicine, Baltimore, MD, United States of America, **3** Genome Resource Center, Institute for Genome Sciences, University of Maryland School of Medicine, Baltimore, MD, United States of America, **4** Department of Pathology, University of Maryland School of Medicine, Baltimore, MD, United States of America, **5** Department of Microbiology and Immunology, University of Maryland School of Medicine, Baltimore, MD, United States of America

* abanerjee@som.umaryland.edu



OPEN ACCESS

Citation: Simpson HM, Khan RZ, Song C, Sharma D, Sadashivaiah K, Furusawa A, et al. (2015) Concurrent Mutations in *ATM* and Genes Associated with Common γ Chain Signaling in Peripheral T Cell Lymphoma. PLoS ONE 10(11): e0141906. doi:10.1371/journal.pone.0141906

Editor: Yan W. Asmann, Mayo Clinic, UNITED STATES

Received: May 15, 2015

Accepted: October 14, 2015

Published: November 4, 2015

Copyright: © 2015 Simpson et al. This is an open access article distributed under the terms of the [Creative Commons Attribution License](http://creativecommons.org/licenses/by/4.0/), which permits unrestricted use, distribution, and reproduction in any medium, provided the original author and source are credited.

Data Availability Statement: All exome sequencing data is available through the NCBI BioProject (accession code SRP047386).

Funding: This work was funded by National Institute of Health grants (P30CA134272, K08HL93207) (AB) (<http://www.nih.gov/>), the Gabrielle's Angel Foundation for Cancer Research (AB) (<http://www.gabriellesangels.org/>), the American Cancer Society (AB) (<http://www.cancer.org/>), and the Marlene and Stewart Greenebaum Cancer Center (<http://umm.edu/programs/cancer>). The funders had no role in

Abstract

Peripheral T cell lymphoma (PTCL) is a heterogeneous malignancy with poor response to current therapeutic strategies and incompletely characterized genetics. We conducted whole exome sequencing of matched PTCL and non-malignant samples from 12 patients, spanning 8 subtypes, to identify potential oncogenic mutations in PTCL. Analysis of the mutations identified using computational algorithms, CHASM, PolyPhen2, PROVEAN, and MutationAssessor to predict the impact of these mutations on protein function and PTCL tumorigenesis, revealed 104 somatic mutations that were selected as high impact by all four algorithms. Our analysis identified recurrent somatic missense or nonsense mutations in 70 genes, 9 of which contained mutations predicted significant by all 4 algorithms: *ATM*, *RUNX1T1*, *WDR17*, *NTRK3*, *TP53*, *TRMT12*, *CACNA2D1*, *INTS8*, and *KCNH8*. We observed somatic mutations in *ATM* (ataxia telangiectasia-mutated) in 5 out of the 12 samples and mutations in the common gamma chain (γ_c) signaling pathway (*JAK3*, *IL2RG*, *STAT5B*) in 3 samples, all of which also harbored mutations in *ATM*. Our findings contribute insights into the genetics of PTCL and suggest a relationship between γ_c signaling and *ATM* in T cell malignancy.

Introduction

Peripheral T cell Lymphoma (PTCL) accounts for 10–15% of Non-Hodgkin's Lymphoma with about 7,000 cases diagnosed per year in the United States [1]. With at least 20 different subtypes currently recognized under WHO classification updated in 2008, PTCL represents a

study design, data collection and analysis, decision to publish, or preparation of the manuscript.

Competing Interests: The authors have declared that no competing interests exist.

heterogeneous group of mature T and NK cell neoplasms with overall poor prognoses [2]. Traditionally, PTCL has been treated similarly to B cell lymphomas with various CHOP (cyclophosphamide, doxorubicin, vincristine, prednisone) based chemotherapy regimens and no targeted therapeutics effective against more than a subset of cases are currently available. While there is variability in outcome based on subtype, reported 5-year overall survival (OS) remains <40% [2, 3]. Recent clinical trials of alternative combinations of cytotoxic chemotherapeutics and newer therapeutic approaches tested thus far, including monoclonal antibodies such as anti-CD52, anti-CD30, and anti-CD4; immunoconjugates such as denileukin diftitox and brentuximab vedotin; epigenetic modifiers including HDAC inhibitors; signaling inhibitors such as Syc and protein kinase C inhibitors; and immunosuppressive (cyclosporine) and immunomodulatory agents (lenalidomide) are promising but have not yet led to substantial improvements in OS for PTCL patients [1, 2, 4]. Thus, there is a critical need for insights from the genomics of PTCL to facilitate the discovery of novel, personalized therapeutic targets and approaches.

To identify oncogenic mutations, and by extension, therapeutic targets in PTCL, recent studies have employed single gene, whole exome, or genome wide sequencing techniques in cases of PTCL [5–16]. These studies have identified mutations in a wide variety of genes including *STAT3*, *STAT5B*, *JAK1*, *JAK3*, *FYN*, *RHOA*, *NOTCH1*, *CD58*, *B2M*, *PLCG1*, *PTPN2*, *EZH2*, *FBXW10*, *TET2*, *DNMT3A*, *IDH2*, *ATM*, *CHEK2*, and p53 related genes (*TP53*, *TP63*, *CDKN2A*, *WWOX*, and *ANKRD11*) in different subtypes of PTCL. Due to the relatively low incidence of PTCL, however, the discovery cohorts within these studies are limited, with relatively small numbers of primary PTCL samples subjected to high throughput sequencing. Given the limited number of PTCL samples sequenced relative to many other cancers, further sequencing studies serve both to validate identified driver mutations and to discover novel mutations. Therefore, it is critical to compare and analyze mutations identified across independent studies to help understand the complete role of oncogenic mutations in PTCL. We conducted whole exome sequencing of 12 PTCL cases from untreated patients, compared to patient-derived non-tumor control cells, to identify somatic mutations: potential oncogenic drivers of PTCL.

Materials and Methods

Primary PTCL specimens

Specimens were collected for this study from patients diagnosed with PTCL at the University of Maryland Greenbaum Cancer Center with the approval of the University of Maryland, Baltimore Institutional Review Board (UMB IRB). Written consent was obtained from all patients involved in the study using a consent procedure approved by the UMB IRB. Documentation of the consent process includes patient, patient study number (samples are de-identified prior to use), principal investigator/designee signature, and date. Pathological samples used for analysis include patient blood, bone marrow, or lymph node tissue (S1 Table). Mononuclear cells were isolated from each specimen by subjecting single cell suspensions to Ficoll gradient centrifugation.

Flow cytometry and cell sorting

Cells were stained with fluorophore-labeled antibodies to cell surface molecules for separation of malignant PTCL and non-malignant cell populations (B cell, monocyte) by flow cytometry and cell sorting. Surface antigens used to distinguish PTCL cells and non-malignant cells included CD2, CD3, CD4, CD5, CD7, CD8, CD14, CD19, CD30, CD45, and CD52 (S1 Table).

All fluorophore-labeled antibodies were purchased from eBioscience. Cell sorting was performed using two-laser FACSAria I or three-laser FACSAria II cell sorters.

Genomic DNA extraction

Cells were washed and resuspended in PBS. After addition of Proteinase K and RNase A (Qiagen), genomic DNA was isolated using a DNeasy kit (Qiagen) per manufacturers' instructions.

Exome sequencing

Sequencing library construction, exome capture, sequencing, and analyses were carried out by the Genomics Resource Center (GRC) within the Institute for Genome Sciences (IGS) at the University of Maryland School of Medicine. Genomic DNA libraries with 7bp molecular barcode indexes were constructed for sequencing on the Illumina platform using the NEBNext[®] DNA Sample Prep Master Mix Set 1 (New England Biolabs, Ipswich, MA). DNA was fragmented with the Covaris E210 focused ultrasonicator (Covaris Woburn, MA), targeting a size of 200bp, and libraries were prepared using a modified version of manufacturer's protocol.

Following library construction, targeted capture was performed with the Agilent SureSelect Human All Exon V4 kit following the manufacturer's protocol. Libraries were pooled so that each received $\frac{1}{4}$ or $\frac{1}{2}$ a lane of sequencing, and were sequenced with an Illumina HiSeq2000 sequencer 100PE run, generating an average of 86.8 million passed-filter reads per sample.

Raw data from the sequencer was processed using Illumina's RTA and CASAVA pipeline software and reads were truncated where the median quality score fell below Q20. Initial alignment to the hg19 human reference genome (GRCh37) using BWA (v0.5.9) was followed by GATK (v1.4.5) for indel realignment and base quality score recalibration and Picard MarkDuplicates to remove artificially duplicated library fragments caused by PCR. The average on-target coverage for all samples was 94.4x and >87% of targets were covered at $\geq 20x$ with fewer than 4% of targeted bases lacking coverage. Somatic variants were predicted using both VarScan (v.2.3.7) and MuTect (v1.1.7). The resulting variant sets were annotated using ANNOVAR (v 2014-11-12). On average, VarScan found 208 somatic variants per sample, while MuTect found 264.

Coverage and filtering for calling algorithms

MuTect uses a coverage cutoff of at least 14 reads in the tumor sample and at least 18 reads in the non-malignant cell sample and pre-applies filters to eliminate false positives. Only the high confidence set of calls that did not fail any of the MuTect filters were included in analysis.

VarScan uses a minimum coverage of 6 reads in the tumor sample and 8 reads in the non-malignant sample. We then applied the processSomatic tool to extract a high confidence set of variants. A somatic variant was considered high confidence if the variant allele frequency of at least 10% in tumor (default) and Fisher's Exact Test P-value was < 0.07 (default) [17]. In addition, a threshold was applied for maximum variant allele frequency in the non-malignant samples, determined by the assessed purity of these samples. A false positive filter was then applied to the high confidence call set to remove any false positive variant calls due to sequencing or alignment related artifacts [17].

All variants called by Mutect and/or VarScan were then filtered by population frequency using the 1000 Genomes Project database to exclude variants with allele frequency > 0.01 in the population [18]. Application of this filter excluded 1% of the calls by Mutect and 18% of the calls by VarScan. A total of 3,137 calls by Mutect and 2,054 calls by VarScan (including mutations identified by both calling algorithms) remained for our analysis.

Algorithms to predict potential cancer driver mutations and impact on protein function

Non-synonymous mutations identified were formatted for analysis according to the websites' instructions and then queried by each of the following computational algorithms: Polyphen2 (Polymorphism Phenotyping v2), PROVEAN (Protein Variation Effect Analyzer), MutationAssessor, and CHASM (Cancer-Specific High-throughput Annotation of Somatic Mutations), accessed at <http://genetics.bwh.harvard.edu/pph2/>, <http://provean.jcvi.org/index.php>, <http://mutationassessor.org/>, and <http://www.craat.us/>, respectively. Indels were only analyzed by PROVEAN, as the other algorithms are equipped only for missense mutation analysis.

Results

Whole exome sequencing of PTCL

To identify potential oncogenic mutations in PTCL, we performed whole exome sequencing of matched tumor and non-malignant DNA samples from 12 untreated patients with PTCL. Eight different PTCL subtypes were represented in our patient cohort, including one patient each with hepatosplenic T cell lymphoma (HSTL), T-cell large granular lymphocytic leukemia (T-LGL), lymphoepithelioid T cell lymphoma (LETL), Alk(+) anaplastic large cell lymphoma (ALCL), adult T-cell leukemia/lymphoma (ATLL), and Sezary Syndrome (SS), and three patients each with T-cell prolymphocytic leukemia (T-PLL) and peripheral T-cell lymphoma not otherwise specified (PTCLnos).

Using two different calling algorithms, Mutect and VarScan, we detected a total of 1,245 unique, high-confidence, non-synonymous SNVs and 59 indels that passed our filters, across the 12 PTCL cases with an average of 93 non-synonymous somatic mutations per PTCL sample (range 15–340). More non-synonymous mutations were independently identified by Mutect (1,110) than VarScan (499); 333 mutations were identified by both calling algorithms. The most common transition/transversion resulting in non-synonymous exonic mutation was G>T+C>A (Fig 1A). The significance of this mutational pattern is not fully understood and other sequencing studies suggest that this transition/transversion is less than half as common as G>A+C>T in a wide variety of cancers [19, 20]. Approximately 71% of the mutations identified by Mutect and VarScan, are missense and nonsense mutations (Fig 1B). Of other mutations identified by the calling algorithms 25% are silent mutations, 1% are splice site mutations, and 13% are mutations in non-translated RNA. In subsequent analysis, we focused on the missense and nonsense mutations in protein coding regions due to their increased likelihood to result in functional protein changes. Silent, non-polymorphic mutations, however, may still affect transcription, translation, mRNA transport, or splicing and if the variant results in the need for a rare tRNA it may delay translation enough to cause the variations in protein folding [21]. We include a list of all recurrent genes with synonymous mutations by subtype that were identified in our patient cohort (S2 Table).

Prediction of functionally important variants in PTCL

To identify the non-synonymous SNVs from our samples most likely to influence protein function, we used three independent structure/homology-based algorithms: Polyphen2 PROVEAN, MutationAssessor, as well as a fourth algorithm, CHASM, designed to prioritize somatic missense mutations based on their representation in large-scale cancer sequencing studies [22–26]. CHASM uses COSMIC (Catalogue of Somatic Mutations in Cancer) as a training set to predict whether a somatic missense mutation will contribute to the tumorigenicity of the malignant cell from which it was sequenced [24]. Of the 1,245 missense SNVs and 59 indels called, 154 (12%) were selected by CHASM as likely to be cancer driver mutations. PolyPhen2 predicts the

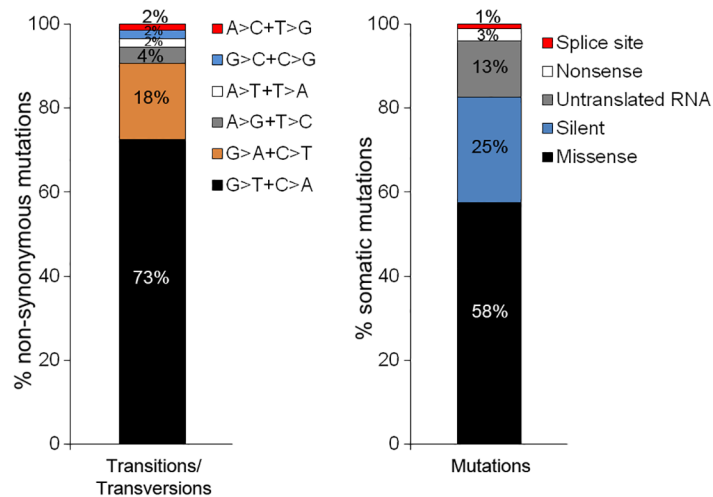


Fig 1. Characterization of somatic mutations in PTCL. (A) Bar graph shows percent of specified transitions and transversions resulting in non-synonymous somatic mutations identified by Mutect and VarScan in PTCL samples. (B) Bar graph shows percentage of each type of somatic mutation identified in PTCL samples.

doi:10.1371/journal.pone.0141906.g001

functional impact of a missense mutation by comparison of 1) biochemical changes in protein structure between the wild-type and mutant allele based on predicted protein domains and 2) sequence homology based on evolutionary conservation of the wild-type allele between species [22]. Of the non-synonymous mutations identified, 52% were predicted to be “Probably Damaging” and 16% to be “Possibly Damaging” to protein function by PolyPhen2 (Fig 2A). MutationAssessor prioritizes relative mammalian evolutionary conservation over conservation between all species, to predict the probability of the mutation significantly impacting mammalian protein function [26]. This more conservative method predicted 8% of the mutations will have a “High” and 35% will have a “Medium” chance of significantly affecting protein

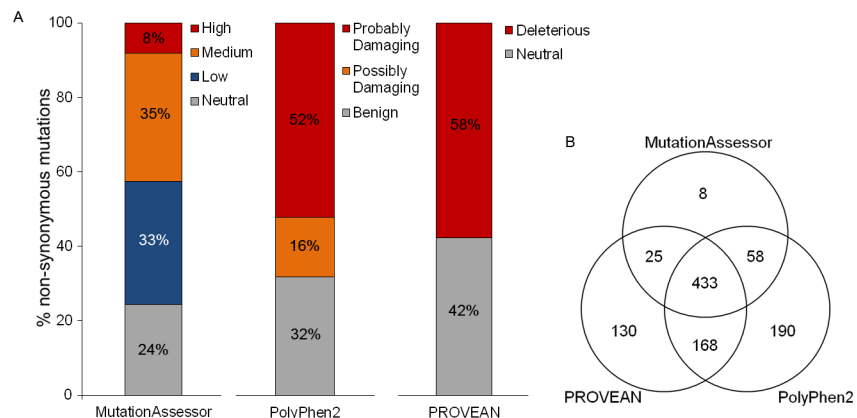


Fig 2. Functional algorithms, MutationAssessor, PolyPhen2, and PROVEAN, predict the majority of somatic mutations identified to significantly impact protein function. (A) Bar graph shows percent of non-synonymous somatic mutations and their probability to impact protein function, as predicted by MutationAssessor, PolyPhen2, and PROVEAN. (B) Venn diagram shows number of non-synonymous somatic mutations predicted to significantly impact protein function by each algorithm or combination of algorithms: MutationAssessor, PolyPhen2, and PROVEAN. Mutations were considered significant if selected as “high” or “medium”, “probably damaging” or “possibly damaging,” and “deleterious,” respectively.

doi:10.1371/journal.pone.0141906.g002

functions (Fig 2A). PROVEAN compares homologous sequences, including the region surrounding substituted, added, or deleted amino acids, so that it may assess the potential for deleterious impact of SNVs and indels on protein function [23]. Of the SNVs and indels analyzed, 58% were predicted to be “Deleterious” using this algorithm (Fig 2A). Of the 1,245 SNVs, 433 SNVs were predicted by all three general algorithms, Polyphen2, PROVEAN, and MutationAssessor, to encode functionally relevant amino acid changes (Fig 2B). Of these, 104 were also selected by CHASM as likely to be cancer drivers (Table 1).

Genes containing non-synonymous somatic mutations in multiple PTCL samples

We identified 70 genes with missense or nonsense somatic mutations in more than one PTCL sample. For each of these genes, we determined whether the SNVs identified were predicted to have functional consequences by the Polyphen2, PROVEAN, MutationAssessor, or CHASM algorithms (Fig 3A). The most frequently mutated gene in our sample cohort is *ATM*, found to contain non-synonymous somatic mutations in 5 out of the 12 samples (42%). *ATM* has previously been shown to harbor somatic mutations in over 50% of sequenced tumor samples from patients with the T-PLL subtype of PTCL [12, 33–36]. Out of the 5 samples with *ATM* mutations in our data, three were from cases of T-PLL and the two others were from HSTL and T-LGL cases. *ATM* mutations in conserved residues were verified by Sanger sequencing (S1 Fig). Mutations in *RUNX1T1* (encoding cyclin-D-related protein, a transcriptional regulator) and *WDR17* (WD repeat-containing protein 17) were identified in 3 patient samples in the cohort and predicted to be likely cancer driver mutations impacting protein function by all 4 algorithms (Fig 3A). Mutations in *TTN* (titin, involved in chromosome segregation) were also identified in 3 samples and predicted to have a significant probability of impacting protein function by Polyphen2, PROVEAN, and MutationAssessor. Mutations in *MUC16* (mucin) were also observed in 3 samples and predicted to be significant by Polyphen2 and PROVEAN. Mutations in *CACNA2D* (a voltage-dependent calcium channel), *INTS8* (a component of small nuclear RNA transcription complex), *KCNH8* (a potassium voltage-gated channel), *NTRK3* (tyrosine-protein kinase receptor), *TP53* (p53), and *TRMT12* (a guanosine modifying transferase) were identified in 2 samples and predicted to be cancer driver mutations impacting protein function by all 4 algorithms (Fig 3A). Twenty of the 70 mutations identified were selected as a representative subset for Sanger sequencing validation, all of which were verified.

Our data contains three samples from patients with T-PLL, all with a mutation in *ATM* and two out of the three with mutations in *CASP8AP2* (CASP8-associated protein 2, TNF α signaling), *CCR8* (chemokine receptor), *DNAH7* (dynein heavy chain), *FEZF1* (fez family zinc finger protein), *INTS8*, *LRP1B* (receptor-mediated endocytosis), *MTMR8* (phosphatase), *MUC16*, *NOP2* (methyltransferase, cell cycle regulation), *RASAL2* (Ras GTPase-activating protein), *RUNX1T1*, *SDK2* (cell adhesion), *SLC13A5* (sodium/citrate cotransporter), *SLC16A14* (mono-carboxylate transporter), *SRRM2* (pre-mRNA splicing), *TNFRSF19* (tumor necrosis factor receptor superfamily member), *TTN*, *UNC79* (sodium channel complex component), and *WDR17* (Fig 3B). Two of the 3 samples from patients with PTCLnos harbor mutations in *PCDHGA11* (a potential calcium-dependent cell-adhesion protein), but we did not identify any other recurrent mutations in this subtype.

Among the 70 genes found to contain somatic mutations in multiple samples, two genes contained identical somatic mutations in two different PTCL samples: TCF12 R300L (transcriptional regulator) and TMEM51 E169del (transmembrane protein) (Fig 3A, in blue; Fig 3B in gold). TCF12 R300L and TMEM51 E169del were predicted to significantly alter function of the protein by PROVEAN. These SNVs have not previously been identified.

Table 1. 104 somatic mutations predicted to be cancer drivers that significantly alter protein function by all four algorithms.

Subtype	Mutation	Subtype	Mutation	Subtype	Mutation	Subtype	Mutation
ALCL	ABCB1 Q475H	T-PLL	ATM C2930F	T-PLL	MYO3A P380H	T-PLL	TBC1D16 R76L
ALCL	EIF3M G112W	T-PLL	ATM R3008H ¹	T-PLL	NEK8 G86C	T-PLL	TBC1D22B P303H
ALCL	RAB13 R79S	T-PLL	CA12 W62C	T-PLL	NMS R69M	T-PLL	TESK2 G136W
ALCL	SLC22A4 G161W	T-PLL	CAMKMT G255W	T-PLL	NT5C1B-RDH14 G353W	T-PLL	TNIK K41N
ALCL	SUSD1 G67W	T-PLL	CAPN6 R454S	T-PLL	OSBP P497Q	T-PLL	TNRC6C W1487C
ALCL	VRK1 W261L	T-PLL	CNPY3 R95L	T-PLL	PCDHB3 R92L	T-PLL	TRIM2 P37H
ALCL	ZFHX4 R2659L	T-PLL	CNTNAP2 R157S	T-PLL	PFN2 R56L	T-PLL	TSTD2 P284Q
ATLL	ADSL G54C	T-PLL	CREBBP R1185S	T-PLL	PIM3 P213Q	T-PLL	UBP1 P142Q
ATLL	ALDOA R60C	T-PLL	CUX1 R1259L	T-PLL	POPDC2 R216L	T-PLL	USP24 P124H
ATLL	DMBX1 R122C	T-PLL	DHX30 R918L	T-PLL	PRC1 P151T	T-PLL	USP4 P798Q
ATLL	KCNH4 R353L	T-PLL	DIAPH2 W643L	T-PLL	PRDM16 R173H	T-PLL	UTRN R3348S
ATLL	MRPS33 R89S	T-PLL	DOCK7 G1343W	T-PLL	PREP W150L	T-PLL	WDR17 W1265L
ATLL	NFATC3 W644C	T-PLL	ERLIN2 R169L	T-PLL	PREX2 W234L	T-PLL	ZBTB39 H556N
ATLL	PRKCB D427N	T-PLL	FAM169A G156W	T-PLL	PTPRD G904V	PTCLnos	CACNA2D1 A248P
HSTL	C4orf27 G130W	T-PLL	FAM219A R35L	T-PLL	RAB6B G25W	PTCLnos	CLPX G296V
HSTL	FKBP4 R359L	T-PLL	FBXL2 W42L	T-PLL	RAE1 W156L	PTCLnos	FBXW7 S464L
LETL	EGR2 H416D	T-PLL	FILIP1 D394G	T-PLL	RBL2 W205L	PTCLnos	FYN G407R
LETL	NTRK3 P331L	T-PLL	HECW1 R1263L	T-PLL	RPN1 G325W	PTCLnos	HIF1A R53L
SS	ESRRG L67H	T-PLL	HTR3A R245C	T-PLL	RUNX1T1 R349L	PTCLnos	INHBA M418T
SS	PCDHGA5 E253K	T-PLL	ICA1 W242L	T-PLL	RUNX1T1 R229L	PTCLnos	KCNH8 Y671C
TLGL	CSNK2A1 R80H	T-PLL	INTS8 W548L	T-PLL	RXR8 R52L	PTCLnos	MAN1C1 P302S
TLGL	PGD R112L	T-PLL	KCNJ6 R214L	T-PLL	SLC35C1 P73T	PTCLnos	MMP24 Y170C
TLGL	RTF1 M199K	T-PLL	KIT W582L	T-PLL	SLC44A4 G525W	PTCLnos	PAPPA2 Q822K
TLGL	SCN2A W386L	T-PLL	LIMK2 G520W	T-PLL	SPTLC3 R533L	PTCLnos	TBC1D22A G306W
TLGL	SERPINA12 P76H	T-PLL	LZTS2 M26I	T-PLL	STRADB P223Q	PTCLnos	TP53 V41M ²
T-PLL	ATG13 W50L	T-PLL	MYO1B R716L	T-PLL	TAF8 G73W	PTCLnos	TRMT12 P60L

CHASM significance determined by $p \leq 0.05$. If a mutation was previously identified, the appropriate citation is listed as a footnote [27–32].

¹ Camacho, et. al. 2002; Navrkalova, et. al. 2013; Biankin, et. al. 2012; Fang, et. al. 2003; Gronbaek, et. al. 2002

² Achatz, et. al. 2007

doi:10.1371/journal.pone.0141906.t001

ATM mutations in PTCL

ATM has been found to be mutated, or deleted, in the majority of cases of T-PLL, with most of the identified mutations clustering near the ATM PI3Kinase domain [12, 35]. Out of the five samples with ATM point mutations in our study, three are from patients with T-PLL, while the final two are from patients with HSTL and T-LGL. Three of the somatic mutations identified, two from T-PLL samples and one from the HSTL sample, are in or near the highly conserved kinase domain (Fig 4). The third T-PLL sample contains mutations in the FAT (FRA-P-ATM-TRRAP) domain adjacent to the kinase domain. The T-LGL case contained a mutation upstream of the FAT domain, outside of the highly conserved region of the protein. Of the mutations, the R3008H mutation has been previously observed in multiple cancers, including pancreatic cancer, chronic lymphocytic leukemia, mantle cell lymphoma, and diffuse large B cell lymphoma and has been shown to decrease expression of ATM in mantle cell lymphoma, suggesting that it is associated with a loss-of-function [28–32]. Furthermore, the R3008 residue has been previously found to be mutated in cases of T-PLL, including a T-PLL case included in our analysis [37]. SNVs and indels within 10 bases of two SNVs we identified, N2435I and

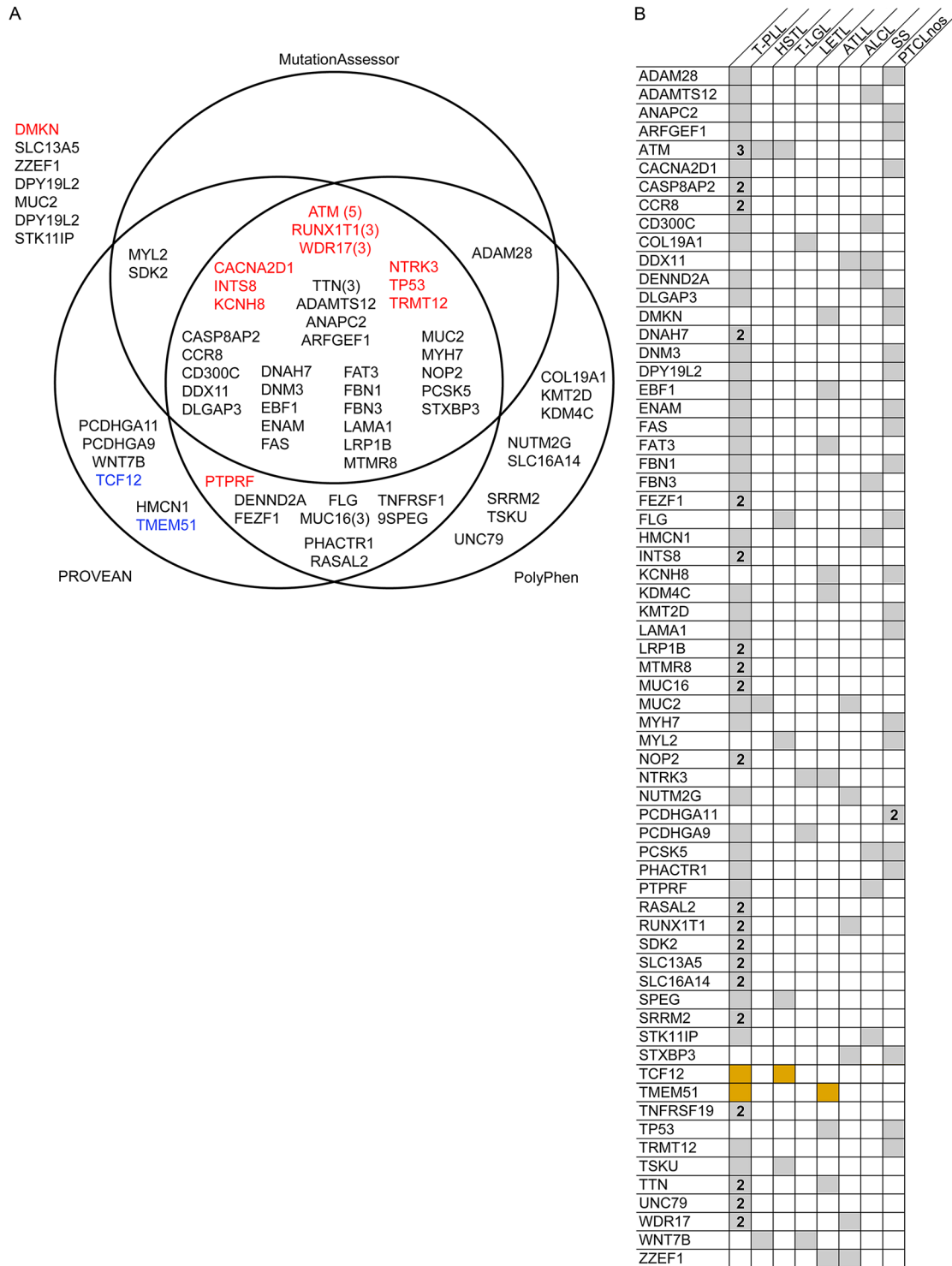


Fig 3. 70 genes contain somatic mutations in more than one PTCL sample. (A) Venn diagram shows which algorithms predicted the mutations in genes somatically mutated in multiple PTCL cases to significantly alter protein function. Genes listed in red contain significant potential cancer driver mutations by CHASM ($p \leq 0.05$). Genes listed in blue contain identical SNVs in both samples. Genes were found to contain mutations in two cases, unless indicated otherwise with a number in parentheses. (B) Grid shows which PTCL subtypes (columns) contain the somatic mutations identified in genes mutated in more than one sample (rows) via grey shaded boxes. Gold shading indicates identical repeated SNVs identified in multiple cases/subtypes. Numbers in boxes indicate the number of samples of the indicated subtype containing a mutation in the indicated gene, if greater than one.

doi:10.1371/journal.pone.0141906.g003

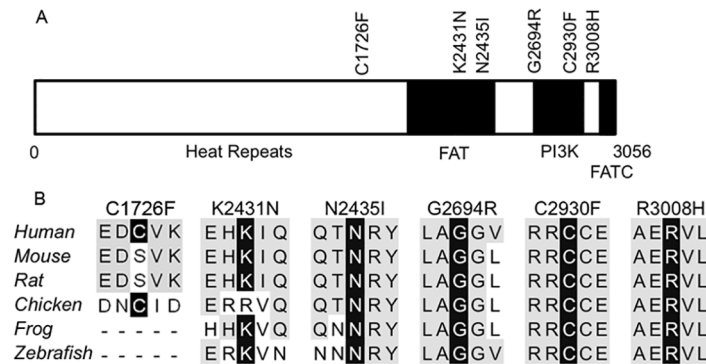


Fig 4. Somatic mutations in ATM, identified in PTCL patients, involve highly conserved residues. (A) Schematic representation of ATM protein domains showing location of somatic mutations in ATM from 5 different PTCL samples. (B) Multiple sequence alignment across species around the 6 mutations in ATM found in 5 samples from patients with PTCL. Conserved mutated residue highlighted in black, other conserved residues highlighted in grey.

doi:10.1371/journal.pone.0141906.g004

K2431N, have been associated with T-PLL as well as B-cell chronic lymphocytic leukemia [34, 38, 39]. In our data, loss-of-ATM-function is supported by the observation of homozygous mutation (loss of heterozygosity) at the *ATM* locus in the three T-PLL samples and all SNVs were predicted to significantly impact ATM protein function by at least one of the algorithms utilized.

As recurrent mutations in ATM and p53 related molecules have been identified in other studies of PTCL, we scanned our data for mutations in this pathway and identified mutations in several related genes: *TP53*, *BRAT1*, *CREBBP*, *MAPK9*, *MAPK14*, *NFKBIA*, and *TLK1*. p53 contained mutations in one case of PTCLnos and one of ATLL, encoding amino acid changes V41M and D10Y, respectively. p53 V41M was predicted to be a cancer driver mutation by CHASM and selected by all three general algorithms as likely to impact protein function.

Common gamma chain (γ_c) signaling pathway mutations in PTCL

JAK/STAT signaling pathway molecules (STAT3, STAT5B, JAK1, and JAK3) have previously been shown to be recurrently mutated in various subtypes of PTCL [5, 7–9, 12]. We observed mutations in three genes important in JAK/STAT signal transduction through the γ_c in our sample set: *IL2RG*, *JAK3*, and *STAT5B*, verified by Sanger sequencing (Fig 5 and S2 Fig).

In one of our samples from a patient with T-PLL we observed a somatic mutation in a conserved region of JAK3 adjacent to the pseudokinase domain, M511I (Fig 5A and 5B). JAK3 M511I has been previously described in T-PLL, SS, acute myeloid leukemia, and T-cell acute lymphoblastic leukemia (T-ALL), and has been characterized as an activating mutation, conferring cytokine independent growth to Ba/F3 cells and demonstrating transforming potential in murine hematopoietic progenitor cells [40–45]. CHASM predicted JAK3 M511I to be a cancer driver mutation (S3 Table).

In the HSTL sample in our analysis, we identified a somatic mutation in a highly conserved residue in the SH2 domain of STAT5B encoding a N642H mutation, a prolific oncogenic mutation found in many hematologic malignancies (Fig 5C and 5D). STAT5 N642H mutation was first identified as an activating mutation in an *in vitro* screen, then demonstrated to increase the transcriptional activity of STAT5A, which shares extensive sequence homology with STAT5B, and shown to allow cytokine independent growth of Ba/F3 cells [46]. STAT5B N642H has further been identified in multiple subtypes of PTCL: 2% of cases of T-LGL, 7/21

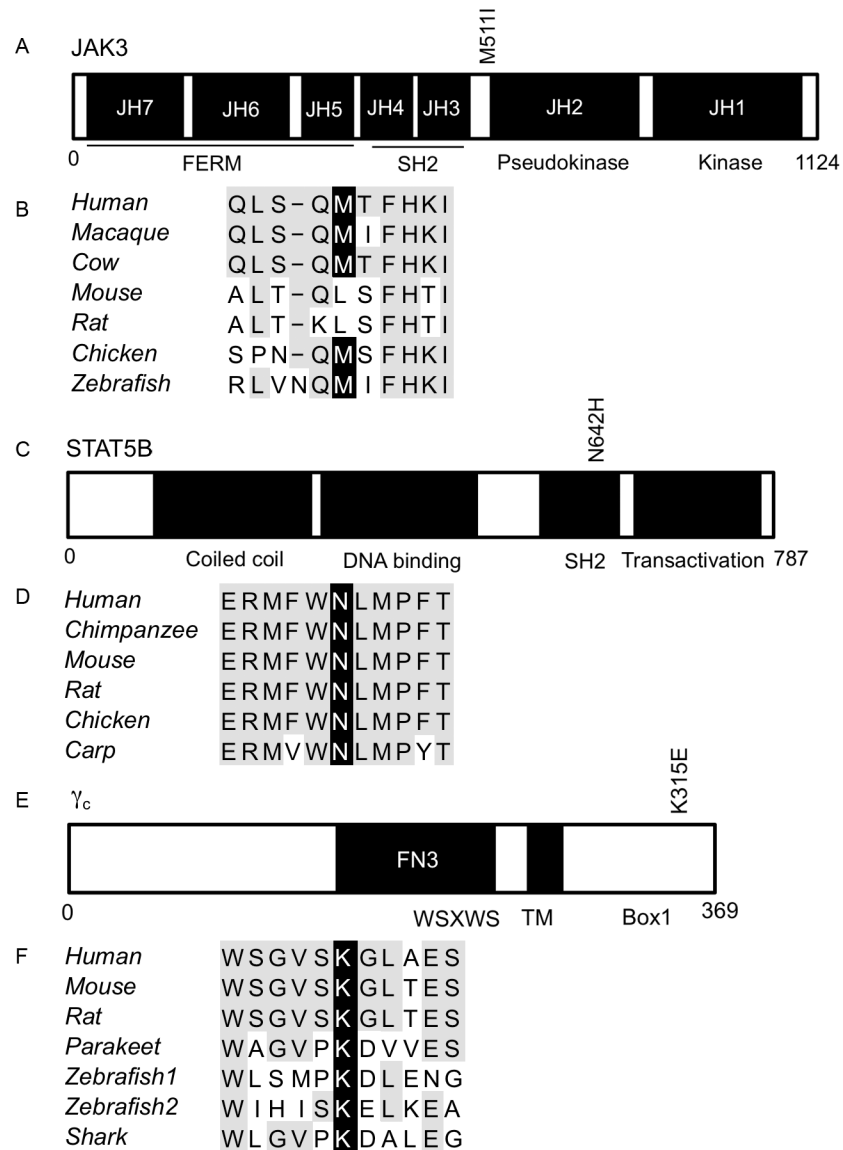


Fig 5. γ_c cytokine signal transducers contain mutations in highly conserved amino acid residues. (A) Schematic representation of JAK3 protein domains showing somatic mutation in identified in PTCL sample. (B) Sequence alignment of JAK3 M511 across 7 species. Conserved mutated residue highlighted in black, other conserved residues in grey. (C) Schematic representation of STAT5B protein domains showing somatic mutation identified in PTCL sample. (D) Sequence alignment of STAT5B N642 across 6 species. Conserved mutated residue highlighted in black, other conserved residues in grey. (E) Schematic representation of γ_c protein domains showing somatic mutation identified in PTCL sample. (F) Sequence alignment of γ_c K315 across 6 species. Conserved mutated residue highlighted in black, other conserved residues in grey.

doi:10.1371/journal.pone.0141906.g005

(33%) of cases of HSTL, and in T-PLL where it has demonstrated increased colony forming capacity in Jurkat cells, a T-cell leukemia cell line [8, 12, 47]. STAT5B N642H has also been found in 6.3% of cases of pediatric T-ALL, correlating with increased risk of relapse and decreased probability of event free survival [48]. Alternative studies do report variation in the rate of STAT5B N642H in pediatric T-ALL: from 1/64 (1.5%) to 1/4 (25%) [49, 50]. This mutation has also been identified in $\gamma\delta$ -T-cell lymphomas where the mutant histidine has been

shown to increase binding affinity for the activating phosphotyrosine, Y699, in the STAT5B molecule leading to persistence of mutant pSTAT5B and increased binding to targets [51]. STAT5B N642H mutation has also been observed in acquired aplastic anemia [52]. PolyPhen2 and PROVEAN predicted this mutation to have a “Probably Damaging” and “Deleterious” impact on the protein, respectively.

The γ_c K315E mutation we observed in a T-PLL case is in a highly conserved residue located in the intracellular region of the γ_c protein C-terminal to the box1 motif, which is required for JAK binding and activation (Fig 5E and 5F). This mutation was recently noted in one other case of T-PLL [12]. PolyPhen2 predicted γ_c K315E to be “Probably Damaging” and MutationAssessor indicated it has a “Medium” probability of having a significant impact on the protein’s function. All three of these γ_c signaling pathway mutations in *IL2RG*, *JAK3*, and *STAT5B* were found in patients who also had mutations in *ATM*. Possible significance of this finding is unknown.

Discussion

Next generation and high throughput sequencing techniques are employed to gain insight into the biology of PTCL in an effort to develop a basis for novel therapeutic approaches. We performed whole exome sequencing of paired PTCL and non-malignant cell DNA from 12 untreated PTCL patients, representing a total of 8 different subtypes, in order to identify potential oncogenic mutations. Some of the mutations we identified in our study overlap with those identified in other current PTCL sequencing studies, lending validity to studies with relatively small sample sizes and supporting the potential importance of genes found to contain mutations in multiple studies in PTCL. Our results support and expand upon current understanding of the role of mutated genes in PTCL to help lay the groundwork for future development of targeted therapeutic strategies.

Somatic mutations in genes encoding molecules involved in cytokine signal transduction, and specifically in γ_c associated JAK-STAT signaling, have previously been identified in NK-/T-cell lymphoma (NKTCL), angioimmunoblastic T-cell lymphoma (AITL), T-PLL, HSTL, SS, and T-LGL subtypes of PTCL [5, 8, 12, 42, 47, 53]. We identified somatic mutations in JAK-STAT signaling molecules associated with γ_c signaling in T-PLL and HSTL. Other sequencing studies have revealed somatic activating mutations in *JAK3* (A572V and A573V) in 38% of NKTCL, *STAT3* and *STAT5B* in T-LGL, and recurrent gain-of-function mutations in *JAK2* and *STAT3* in AITL [5, 8, 42, 53]. The malignant transforming potential of *JAK3* M511I has been shown to be dependent on the expression of the γ_c and to increase with γ_c overexpression [54]. Our study, taken together with recent work identifying the γ_c K315E mutation in T-PLL, as well as an indel in the γ_c that was demonstrated to increase *STAT5* transcriptional activity, establishes a pattern of recurrent mutations in the γ_c in T-PLL that may drive the development of this malignancy [12]. As γ_c cytokine signaling, particularly in the context of IL-2, IL-7, and IL-15 signaling, is critical for T-cell differentiation, apoptosis, survival and proliferation, mutations altering this signal transduction pathway are well placed to potentially drive T cells to a cytokine-independent, malignant phenotype [55, 56]. Studies on PTCL are limited in scope by the relative rarity of the disease and the addition of our findings lends validity to these studies in the field where large validation sets are often unavailable. Our observation of activating mutations in *JAK3* and *STAT5B* in T-PLL and HSTL, along with these prior studies, show that mutations leading to activation of γ_c associated JAK-STAT cytokine signaling pathways are present in at least 5 subtypes of PTCL and may represent a unifying trait in a disease marked by heterogeneity between subtypes.

Identification of gain-of-function mutations in the common gamma chain signaling pathway suggests utility of JAK/STAT pathway inhibitors in PTCL therapy. JAK inhibitors are

currently in development and several are approved for patient use, such as ruxolitinib in the treatment of myelofibrosis and tofacitinib in rheumatoid arthritis [57, 58]. In light of the finding of activating mutations in JAK3 in multiple subtypes of PTCL, including our study, it will be important to investigate the use of these inhibitors for the treatment of these malignancies [42, 59]. Furthermore, STAT molecules have been shown to be constitutively activated in some hematologic malignancies, including STAT5 in several subtypes of PTCL, ~35% of cases of HSTL, 2% of T-LGL, and ~6% of pediatric T-ALL often leading to worse patient outcomes [8, 12, 47, 48]. As such, direct inhibition of STATs, such as with pimozide, may be an appealing therapeutic strategy as well [60]. Our results, in combination with the literature, support further investigation of the utility of JAK/STAT pathway inhibitors as a novel therapeutic intervention in PTCL.

The most frequently recurring mutated gene identified in our study is *ATM*, mutated in 5 out of 12 PTCL cases and predicted by algorithms as likely to impact protein function and drive oncogenesis. Another recent whole exome sequencing study of 12 PTCL samples also identified recurrent mutations in *ATM* [11]. One of the *ATM* mutations identified is R3008H, also found in our study, and included in the COSMIC database due to its known association with cancer. Cells with inactivating mutations in *ATM* can be selectively targeted with poly (ADP ribose) polymerase (PARP) inhibitor therapy [61]. PARP inhibitors, such as olaparib, are already in clinical use for treatment of solid tumors and in clinical trials for patients with chronic lymphocytic leukemia and T-PLL and could prove useful for treatment of many other malignancies driven by *ATM* deficiency. Furthermore, the three PTCL samples (two T-PLL, one HSTL) with mutations in γ_c signal transduction components in our study were among the samples containing mutations in *ATM*. Our study suggests that, due to overlap of mutations in *ATM* and the γ_c signaling pathway, there is a possible correlation between these two pathways in HSTL as well as T-PLL. In a study of HPV viral replication in hepatocytes, phosphorylated STAT5B was found to activate the *ATM* pathway through the action of peroxisome proliferator-activated receptor gamma (PPAR γ) [62]. The mechanisms of the relationships between these pathways have not been explored in hematologic cancers or normal T-cell biology.

Our analysis has identified mutations in several of the highly recurrent mutated genes found in previous PTCL sequencing studies, supporting the importance of these pathways in PTCL oncogenesis. Aside from mutations in *ATM*, p53, and the γ_c signaling pathway, we also identified mutations in *FYN* kinase, *NOTCH* molecules, *RHOA* related molecules, and *PLCG1*, corroborating data published by several other studies [10, 11, 13, 14, 16]. The *FYN* G407R mutation we identified was predicted to be a cancer driver with a significant impact on protein function by all 4 algorithms. Although our data did not contain a mutation in *NOTCH1* or *RHOA*, we did find *NOTCH2*, *NOTCH4*, *RHOV* and *RHOBTB1* mutations, significant by PolyPhen2 and PROVEAN. We also identified a *PLCG1* mutation, P658Q, likely to affect protein function by all 3 general algorithms. These findings are consistent with these other studies in the field, which are also relatively small scope, lending validity to our analysis. Because many PTCL studies are limited by the rarity of the disease, inter-study comparison can help address issues of interpretation of a small study when validation sets are unavailable and demonstrate novel, related somatic mutations in PTCL that may be drivers of PTCL oncogenesis.

We also identified recurrent mutations in *MUC16* and *TTN*. However, these genes have been found to be recurrently mutated in many different whole exome sequencing studies as they are quite long (22,152 and 34,350 amino acids, respectively) and therefore have an increased tendency to accumulate more variants [63]. Thus, despite being selected by the algorithms, we consider these mutations unlikely to be cancer drivers of PTCL.

We used four algorithms, PROVEAN, MutationAssessor, PolyPhen2, and CHASM, as a tool to predict mutations that have a higher chance of driving PTCL oncogenesis [22–26]. Our analysis suggests that while algorithms may be useful in identifying mutations with a significant impact on protein function and tumorigenesis, mutations should not necessarily be dismissed from consideration as cancer drivers if not selected by these algorithms. It is possible that these computational programs are not as powerful in the identification of activating mutations, as JAK3 M511I and STAT5B N642H mutations were each predicted to be significant by only one of the algorithms, even though they have been previously characterized as activating mutations capable of inducing cytokine independent cell growth [41–44, 46]. These programs are most useful in conjunction with other methods of predicting PTCL critical mutations, such as identification of recurrent mutations in known cancer pathways or genes mutated in other related cancers.

Publication of our data set will enable inclusion of the whole exome sequencing data from these primary PTCL patient samples in future research and analysis. Further assessments using this data, such as to determine copy number variation (CNV), may yield more insights into potential cancer drivers and therapeutic strategies. CNVs are important sources of genetic variation that involve significantly larger areas of the genome than SNVs and may lead to oncogenic phenotypes. Generally, CNV calling in exome data is more challenging and error prone than in whole genome sequencing and is still further complicated by complexity of tumor genomes. Recently developed tools to improve the accuracy of assessing CNVs in exome sequencing data, such as PatternCNV, may have utility in further identifying PTCL driver variations in the genomes of malignant T cells in this data set [64].

Our study, together with prior findings, expand the total number of PTCL samples analyzed for somatic mutations so that less common mutations identified in one study, such as γ_c K315E, may be exposed as recurrent, potentially critical mutations in the process of PTCL tumorigenesis and its relationship to normal T-cell biology to pave the way for the discovery and development of novel therapeutic targets.

Supporting Information

S1 Fig. Sanger sequencing chromatograms of γ_c signaling pathway transducers verify SNVs identified by whole exome sequencing.

(TIF)

S2 Fig. Sanger sequencing chromatograms of ATM verify SNVs identified by whole exome sequencing.

(TIF)

S1 Table. Descriptions of PTCL patient pathological samples.

(TIF)

S2 Table. Recurrent synonymous mutations identified in primary PTCL cases by subtype.

(TIF)

S3 Table. Somatic mutations identified in primary PTCL cases predicted to be oncogenic driver mutations by CHASM.

(TIF)

Acknowledgments

This work was supported by National Institute of Health grants (P30CA134272, K08HL93207), the Gabrielle's Angel Foundation for Cancer Research, the American Cancer

Society and the Marlene and Stewart Greenebaum Cancer Center. Cell sorting was performed at the Marlene and Stewart Greenebaum Cancer Center Flow Cytometry Shared Service.

Author Contributions

Conceived and designed the experiments: HMS RZK AB. Performed the experiments: HMS RZK CS DS KS NS AF APR AK AB. Analyzed the data: HMS RZK LJT XL QCC LS AB. Contributed reagents/materials/analysis tools: LJT XL QCC SN LS FL APR AK AB. Wrote the paper: HMS RZK AB.

References

1. Intlekofer AM, Younes A. From empiric to mechanism-based therapy for peripheral T cell lymphoma. *Int J Hematol*. 2014 Mar; 99(3):249–62. doi: [10.1007/s12185-014-1521-2](https://doi.org/10.1007/s12185-014-1521-2) PMID: [24510453](https://pubmed.ncbi.nlm.nih.gov/24510453/)
2. Foss FM, Zinzani PL, Vose JM, Gascoyne RD, Rosen ST, Tobinai K. Peripheral T-cell lymphoma. *Blood*. 2011 Jun 23; 117(25):6756–67. doi: [10.1182/blood-2010-05-231548](https://doi.org/10.1182/blood-2010-05-231548) PMID: [21493798](https://pubmed.ncbi.nlm.nih.gov/21493798/)
3. Savage KJ. Update: peripheral T-cell lymphomas. *Curr Hematol Malig Rep*. 2011 Dec; 6(4):222–30. doi: [10.1007/s11899-011-0100-3](https://doi.org/10.1007/s11899-011-0100-3) PMID: [21953415](https://pubmed.ncbi.nlm.nih.gov/21953415/)
4. Skarbnik AP, Burki M, Pro B. Peripheral T-cell lymphomas: a review of current approaches and hopes for the future. *Front Oncol*. 2013; 3:138. doi: [10.3389/fonc.2013.00138](https://doi.org/10.3389/fonc.2013.00138) PMID: [23755375](https://pubmed.ncbi.nlm.nih.gov/23755375/)
5. Koskela HL, Eldfors S, Ellonen P, van Adrichem AJ, Kuusanmaki H, Andersson EI, et al. Somatic STAT3 mutations in large granular lymphocytic leukemia. *N Engl J Med*. 2012 May 17; 366(20):1905–13. doi: [10.1056/NEJMoa1114885](https://doi.org/10.1056/NEJMoa1114885) PMID: [22591296](https://pubmed.ncbi.nlm.nih.gov/22591296/)
6. Vasmatazis G, Johnson SH, Knudson RA, Ketterling RP, Braggio E, Fonseca R, et al. Genome-wide analysis reveals recurrent structural abnormalities of TP63 and other p53-related genes in peripheral T-cell lymphomas. *Blood*. 2012 Sep 13; 120(11):2280–9. doi: [10.1182/blood-2012-03-419937](https://doi.org/10.1182/blood-2012-03-419937) PMID: [22855598](https://pubmed.ncbi.nlm.nih.gov/22855598/)
7. Jerez A, Clemente MJ, Makishima H, Koskela H, Leblanc F, Peng Ng K, et al. STAT3 mutations unify the pathogenesis of chronic lymphoproliferative disorders of NK cells and T-cell large granular lymphocyte leukemia. *Blood*. 2012 Oct 11; 120(15):3048–57. doi: [10.1182/blood-2012-06-435297](https://doi.org/10.1182/blood-2012-06-435297) PMID: [22859607](https://pubmed.ncbi.nlm.nih.gov/22859607/)
8. Rajala HL, Eldfors S, Kuusanmaki H, van Adrichem AJ, Olson T, Lagstrom S, et al. Discovery of somatic STAT5b mutations in large granular lymphocytic leukemia. *Blood*. 2013 May 30; 121(22):4541–50. doi: [10.1182/blood-2012-12-474577](https://doi.org/10.1182/blood-2012-12-474577) PMID: [23596048](https://pubmed.ncbi.nlm.nih.gov/23596048/)
9. Huang Y, de Reynies A, de Leval L, Ghazi B, Martin-Garcia N, Travert M, et al. Gene expression profiling identifies emerging oncogenic pathways operating in extranodal NK/T-cell lymphoma, nasal type. *Blood*. 2010 Feb 11; 115(6):1226–37. doi: [10.1182/blood-2009-05-221275](https://doi.org/10.1182/blood-2009-05-221275) PMID: [19965620](https://pubmed.ncbi.nlm.nih.gov/19965620/)
10. Shimizu D, Taki T, Utsunomiya A, Nakagawa H, Nomura K, Matsumoto Y, et al. Detection of NOTCH1 mutations in adult T-cell leukemia/lymphoma and peripheral T-cell lymphoma. *Int J Hematol*. 2007 Apr; 85(3):212–8. PMID: [17483057](https://pubmed.ncbi.nlm.nih.gov/17483057/)
11. Palomero T, Couronne L, Khiabanian H, Kim MY, Ambesi-Impiombato A, Perez-Garcia A, et al. Recurrent mutations in epigenetic regulators, RHOA and FYN kinase in peripheral T cell lymphomas. *Nat Genet*. 2014 Feb; 46(2):166–70. doi: [10.1038/ng.2873](https://doi.org/10.1038/ng.2873) PMID: [24413734](https://pubmed.ncbi.nlm.nih.gov/24413734/)
12. Kiel MJ, Velusamy T, Rolland D, Sahasrabudhe AA, Chung F, Bailey NG, et al. Integrated genomic sequencing reveals mutational landscape of T-cell prolymphocytic leukemia. *Blood*. 2014 May 13; 124(9):1460–72. doi: [10.1182/blood-2014-03-559542](https://doi.org/10.1182/blood-2014-03-559542) PMID: [24825865](https://pubmed.ncbi.nlm.nih.gov/24825865/)
13. Manso R, Sanchez-Beato M, Monsalvo S, Gomez S, Cereceda L, Llamas P, et al. The RHOA G17V gene mutation occurs frequently in peripheral T-cell lymphoma and is associated with a characteristic molecular signature. *Blood*. 2014 May 1; 123(18):2893–4. doi: [10.1182/blood-2014-02-555946](https://doi.org/10.1182/blood-2014-02-555946) PMID: [24786457](https://pubmed.ncbi.nlm.nih.gov/24786457/)
14. Nakamoto-Matsubara R, Sakata-Yanagimoto M, Enami T, Yoshida K, Yanagimoto S, Shiozawa Y, et al. Detection of the G17V RHOA mutation in angioimmunoblastic T-cell lymphoma and related lymphomas using quantitative allele-specific PCR. *PLoS One*. 2014; 9(10):e109714. doi: [10.1371/journal.pone.0109714](https://doi.org/10.1371/journal.pone.0109714) PMID: [25310466](https://pubmed.ncbi.nlm.nih.gov/25310466/)
15. Kleppe M, Tousseyn T, Geissinger E, Kalender Atak Z, Aerts S, Rosenwald A, et al. Mutation analysis of the tyrosine phosphatase PTPN2 in Hodgkin's lymphoma and T-cell non-Hodgkin's lymphoma. *Haematologica*. 2011 Nov; 96(11):1723–7. doi: [10.3324/haematol.2011.041921](https://doi.org/10.3324/haematol.2011.041921) PMID: [21791476](https://pubmed.ncbi.nlm.nih.gov/21791476/)

16. Manso R, Rodriguez-Pinilla SM, Gonzalez-Rincon J, Gomez S, Monsalvo S, Llamas P, et al. Recurrent presence of the PLCG1 S345F mutation in nodal peripheral T-cell lymphomas. *Haematologica*. 2015 Jan; 100(1):e25–7. doi: [10.3324/haematol.2014.113696](https://doi.org/10.3324/haematol.2014.113696) PMID: [25304611](https://pubmed.ncbi.nlm.nih.gov/25304611/)
17. Koboldt DC, Zhang Q, Larson DE, Shen D, McLellan MD, Lin L, et al. VarScan 2: somatic mutation and copy number alteration discovery in cancer by exome sequencing. *Genome Res*. 2012 Mar; 22(3):568–76. doi: [10.1101/gr.129684.111](https://doi.org/10.1101/gr.129684.111) PMID: [22300766](https://pubmed.ncbi.nlm.nih.gov/22300766/)
18. Abecasis GR, Altshuler D, Auton A, Brooks LD, Durbin RM, Gibbs RA, et al. A map of human genome variation from population-scale sequencing. *Nature*. 2010 Oct 28; 467(7319):1061–73. doi: [10.1038/nature09534](https://doi.org/10.1038/nature09534) PMID: [20981092](https://pubmed.ncbi.nlm.nih.gov/20981092/)
19. Greenman C, Stephens P, Smith R, Dalgliesh GL, Hunter C, Bignell G, et al. Patterns of somatic mutation in human cancer genomes. *Nature*. 2007 Mar 8; 446(7132):153–8. PMID: [17344846](https://pubmed.ncbi.nlm.nih.gov/17344846/)
20. Kandath C, McLellan MD, Vandin F, Ye K, Niu B, Lu C, et al. Mutational landscape and significance across 12 major cancer types. *Nature*. 2013 Oct 17; 502(7471):333–9. doi: [10.1038/nature12634](https://doi.org/10.1038/nature12634) PMID: [24132290](https://pubmed.ncbi.nlm.nih.gov/24132290/)
21. Kimchi-Sarfaty C, Oh JM, Kim IW, Sauna ZE, Calcagno AM, Ambudkar SV, et al. A "silent" polymorphism in the MDR1 gene changes substrate specificity. *Science*. 2007 Jan 26; 315(5811):525–8. PMID: [17185560](https://pubmed.ncbi.nlm.nih.gov/17185560/)
22. Adzhubei IA, Schmidt S, Peshkin L, Ramensky VE, Gerasimova A, Bork P, et al. A method and server for predicting damaging missense mutations. *Nat Methods*. 2010 Apr; 7(4):248–9. doi: [10.1038/nmeth0410-248](https://doi.org/10.1038/nmeth0410-248) PMID: [20354512](https://pubmed.ncbi.nlm.nih.gov/20354512/)
23. Choi Y, Sims GE, Murphy S, Miller JR, Chan AP. Predicting the functional effect of amino acid substitutions and indels. *PLoS One*. 2012; 7(10):e46688. doi: [10.1371/journal.pone.0046688](https://doi.org/10.1371/journal.pone.0046688) PMID: [23056405](https://pubmed.ncbi.nlm.nih.gov/23056405/)
24. Wong WC, Kim D, Carter H, Diekhans M, Ryan MC, Karchin R. CHASM and SNVBox: toolkit for detecting biologically important single nucleotide mutations in cancer. *Bioinformatics*. 2011 Aug 1; 27(15):2147–8. doi: [10.1093/bioinformatics/btr357](https://doi.org/10.1093/bioinformatics/btr357) PMID: [21685053](https://pubmed.ncbi.nlm.nih.gov/21685053/)
25. Carter H, Samayoa J, Hruban RH, Karchin R. Prioritization of driver mutations in pancreatic cancer using cancer-specific high-throughput annotation of somatic mutations (CHASM). *Cancer Biol Ther*. 2010 Sep 15; 10(6):582–7. PMID: [20581473](https://pubmed.ncbi.nlm.nih.gov/20581473/)
26. Reva B, Antipin Y, Sander C. Predicting the functional impact of protein mutations: application to cancer genomics. *Nucleic Acids Res*. 2011 Sep 1; 39(17):e118. doi: [10.1093/nar/gkr407](https://doi.org/10.1093/nar/gkr407) PMID: [21727090](https://pubmed.ncbi.nlm.nih.gov/21727090/)
27. Achatz MI, Olivier M, Le Calvez F, Martel-Planche G, Lopes A, Rossi BM, et al. The TP53 mutation, R337H, is associated with Li-Fraumeni and Li-Fraumeni-like syndromes in Brazilian families. *Cancer Lett*. 2007 Jan 8; 245(1–2):96–102. PMID: [16494995](https://pubmed.ncbi.nlm.nih.gov/16494995/)
28. Biankin AV, Waddell N, Kassahn KS, Gingras MC, Muthuswamy LB, Johns AL, et al. Pancreatic cancer genomes reveal aberrations in axon guidance pathway genes. *Nature*. 2012 Nov 15; 491(7424):399–405. doi: [10.1038/nature11547](https://doi.org/10.1038/nature11547) PMID: [23103869](https://pubmed.ncbi.nlm.nih.gov/23103869/)
29. Camacho E, Hernandez L, Hernandez S, Tort F, Bellosillo B, Bea S, et al. ATM gene inactivation in mantle cell lymphoma mainly occurs by truncating mutations and missense mutations involving the phosphatidylinositol-3 kinase domain and is associated with increasing numbers of chromosomal imbalances. *Blood*. 2002 Jan 1; 99(1):238–44. PMID: [11756177](https://pubmed.ncbi.nlm.nih.gov/11756177/)
30. Navrkalova V, Sebejova L, Zemanova J, Kminkova J, Kubsova B, Malcikova J, et al. ATM mutations uniformly lead to ATM dysfunction in chronic lymphocytic leukemia: application of functional test using doxorubicin. *Haematologica*. 2013 Jul; 98(7):1124–31. doi: [10.3324/haematol.2012.081620](https://doi.org/10.3324/haematol.2012.081620) PMID: [23585524](https://pubmed.ncbi.nlm.nih.gov/23585524/)
31. Gronbaek K, Worm J, Ralfkiaer E, Ahrenkiel V, Hokland P, Guldborg P. ATM mutations are associated with inactivation of the ARF-TP53 tumor suppressor pathway in diffuse large B-cell lymphoma. *Blood*. 2002 Aug 15; 100(4):1430–7. PMID: [12149228](https://pubmed.ncbi.nlm.nih.gov/12149228/)
32. Fang NY, Greiner TC, Weisenburger DD, Chan WC, Vose JM, Smith LM, et al. Oligonucleotide microarrays demonstrate the highest frequency of ATM mutations in the mantle cell subtype of lymphoma. *Proc Natl Acad Sci U S A*. 2003 Apr 29; 100(9):5372–7. PMID: [12697903](https://pubmed.ncbi.nlm.nih.gov/12697903/)
33. Stilgenbauer S, Schaffner C, Litterst A, Liebisch P, Gilad S, Bar-Shira A, et al. Biallelic mutations in the ATM gene in T-prolymphocytic leukemia. *Nat Med*. 1997 Oct; 3(10):1155–9. PMID: [9334731](https://pubmed.ncbi.nlm.nih.gov/9334731/)
34. Vorechovsky I, Luo L, Dyer MJ, Catovsky D, Amlot PL, Yaxley JC, et al. Clustering of missense mutations in the ataxia-telangiectasia gene in a sporadic T-cell leukaemia. *Nat Genet*. 1997 Sep; 17(1):96–9. PMID: [9288106](https://pubmed.ncbi.nlm.nih.gov/9288106/)
35. Stankovic T, Stewart GS, Byrd P, Fegan C, Moss PA, Taylor AM. ATM mutations in sporadic lymphoid tumours. *Leuk Lymphoma*. 2002 Aug; 43(8):1563–71. PMID: [12400598](https://pubmed.ncbi.nlm.nih.gov/12400598/)
36. Stoppa-Lyonnet D, Soulier J, Lauge A, Dastot H, Garand R, Sigaux F, et al. Inactivation of the ATM gene in T-cell prolymphocytic leukemias. *Blood*. 1998 May 15; 91(10):3920–6. PMID: [9573030](https://pubmed.ncbi.nlm.nih.gov/9573030/)

37. Yuille MA, Coignet LJ, Abraham SM, Yaqub F, Luo L, Matutes E, et al. ATM is usually rearranged in T-cell prolymphocytic leukaemia. *Oncogene*. 1998 Feb 12; 16(6):789–96. PMID: [9488043](#)
38. Stankovic T, Kidd AM, Sutcliffe A, McGuire GM, Robinson P, Weber P, et al. ATM mutations and phenotypes in ataxia-telangiectasia families in the British Isles: expression of mutant ATM and the risk of leukemia, lymphoma, and breast cancer. *Am J Hum Genet*. 1998 Feb; 62(2):334–45. PMID: [9463314](#)
39. Bullrich F, Rasio D, Kitada S, Starostik P, Kipps T, Keating M, et al. ATM mutations in B-cell chronic lymphocytic leukemia. *Cancer Res*. 1999 Jan 1; 59(1):24–7. PMID: [9892178](#)
40. Vaque JP, Gomez-Lopez G, Monsalvez V, Varela I, Martinez N, Perez C, et al. PLCG1 mutations in cutaneous T-cell lymphomas. *Blood*. 2014 Mar 27; 123(13):2034–43. doi: [10.1182/blood-2013-05-504308](#) PMID: [24497536](#)
41. Zhang J, Ding L, Holmfeldt L, Wu G, Heatley SL, Payne-Turner D, et al. The genetic basis of early T-cell precursor acute lymphoblastic leukaemia. *Nature*. 2012 Jan 12; 481(7380):157–63. doi: [10.1038/nature10725](#) PMID: [22237106](#)
42. Koo GC, Tan SY, Tang T, Poon SL, Allen GE, Tan L, et al. Janus kinase 3-activating mutations identified in natural killer/T-cell lymphoma. *Cancer Discov*. 2012 Jul; 2(7):591–7. doi: [10.1158/2159-8290.CD-12-0028](#) PMID: [22705984](#)
43. Bergmann AK, Schneppenheim S, Seifert M, Betts MJ, Haake A, Lopez C, et al. Recurrent mutation of JAK3 in T-cell prolymphocytic leukemia. *Genes Chromosomes Cancer*. 2014 Apr; 53(4):309–16. doi: [10.1002/gcc.22141](#) PMID: [24446122](#)
44. Yamashita Y, Yuan J, Suetake I, Suzuki H, Ishikawa Y, Choi YL, et al. Array-based genomic resequencing of human leukemia. *Oncogene*. 2010 Jun 24; 29(25):3723–31. doi: [10.1038/onc.2010.117](#) PMID: [20400977](#)
45. Degryse S, de Bock CE, Cox L, Demeyer S, Gielen O, Mentens N, et al. JAK3 mutants transform hematopoietic cells through JAK1 activation, causing T-cell acute lymphoblastic leukemia in a mouse model. *Blood*. 2014 Nov 13; 124(20):3092–100. doi: [10.1182/blood-2014-04-566687](#) PMID: [25193870](#)
46. Ariyoshi K, Nosaka T, Yamada K, Onishi M, Oka Y, Miyajima A, et al. Constitutive activation of STAT5 by a point mutation in the SH2 domain. *J Biol Chem*. 2000 Aug 11; 275(32):24407–13. PMID: [10823841](#)
47. Nicolae A, Xi L, Pittaluga S, Abdullaev Z, Pack SD, Chen J, et al. Frequent STAT5B mutations in gamma-delta hepatosplenic T-cell lymphomas. *Leukemia*. 2014 Jun 20.
48. Bandapalli OR, Schuessele S, Kunz JB, Rausch T, Stutz AM, Tal N, et al. The activating STAT5B N642H mutation is a common abnormality in pediatric T-cell acute lymphoblastic leukemia and confers a higher risk of relapse. *Haematologica*. 2014 Oct; 99(10):e188–92. doi: [10.3324/haematol.2014.104992](#) PMID: [24972766](#)
49. Ma X, Wen L, Wu L, Wang Q, Yao H, Ma L, et al. Rare occurrence of a STAT5B N642H mutation in adult T-cell acute lymphoblastic leukemia. *Cancer Genet*. 2015 Jan-Feb; 208(1–2):52–3. doi: [10.1016/j.cancergen.2014.12.001](#) PMID: [25749351](#)
50. Kontro M, Kuusanmaki H, Eldfors S, Burmeister T, Andersson EI, Bruserud O, et al. Novel activating STAT5B mutations as putative drivers of T-cell acute lymphoblastic leukemia. *Leukemia*. 2014 Aug; 28(8):1738–42. doi: [10.1038/leu.2014.89](#) PMID: [24573384](#)
51. Kucuk C, Jiang B, Hu X, Zhang W, Chan JK, Xiao W, et al. Activating mutations of STAT5B and STAT3 in lymphomas derived from gamma-delta-T or NK cells. *Nat Commun*. 2015; 6:6025. doi: [10.1038/ncomms7025](#) PMID: [25586472](#)
52. Babushok DV, Perdignes N, Perin JC, Olson TS, Ye W, Roth JJ, et al. Emergence of clonal hematopoiesis in the majority of patients with acquired aplastic anemia. *Cancer Genet*. 2015 Feb 2.
53. Odejide O, Weigert O, Lane AA, Toscano D, Lunning MA, Kopp N, et al. A targeted mutational landscape of angioimmunoblastic T-cell lymphoma. *Blood*. 2014 Feb 27; 123(9):1293–6. doi: [10.1182/blood-2013-10-531509](#) PMID: [24345752](#)
54. Agarwal A, MacKenzie RJ, Eide CA, Davare MA, Watanabe-Smith K, Tognon CE, et al. Functional RNAi screen targeting cytokine and growth factor receptors reveals oncorequisite role for interleukin-2 gamma receptor in JAK3-mutation-positive leukemia. *Oncogene*. 2014 Aug 11.
55. Lindemann MJ, Benczik M, Gaffen SL. Anti-apoptotic signaling by the interleukin-2 receptor reveals a function for cytoplasmic tyrosine residues within the common gamma (gamma c) receptor subunit. *J Biol Chem*. 2003 Mar 21; 278(12):10239–49. PMID: [12525482](#)
56. Yamane H, Paul WE. Cytokines of the gamma(c) family control CD4+ T cell differentiation and function. *Nat Immunol*. 2012 Nov; 13(11):1037–44. doi: [10.1038/ni.2431](#) PMID: [23080204](#)
57. Thoma G, Druckes P, Zerwes HG. Selective inhibitors of the Janus kinase Jak3—Are they effective? *Bioorg Med Chem Lett*. 2014 Oct 1; 24(19):4617–21. doi: [10.1016/j.bmcl.2014.08.046](#) PMID: [25217444](#)

58. Scott LM, Gandhi MK. Deregulated JAK/STAT signalling in lymphomagenesis, and its implications for the development of new targeted therapies. *Blood Rev.* 2015 Jun 11.
59. Huang Y, de Leval L, Gaulard P. Molecular underpinning of extranodal NK/T-cell lymphoma. *Best Pract Res Clin Haematol.* 2013 Mar; 26(1):57–74. doi: [10.1016/j.beha.2013.04.006](https://doi.org/10.1016/j.beha.2013.04.006) PMID: [23768641](https://pubmed.ncbi.nlm.nih.gov/23768641/)
60. Nelson EA, Walker SR, Xiang M, Weisberg E, Bar-Natan M, Barrett R, et al. The STAT5 Inhibitor Pimozide Displays Efficacy in Models of Acute Myelogenous Leukemia Driven by FLT3 Mutations. *Genes Cancer.* 2012 Jul; 3(7–8):503–11. doi: [10.1177/1947601912466555](https://doi.org/10.1177/1947601912466555) PMID: [23264850](https://pubmed.ncbi.nlm.nih.gov/23264850/)
61. Weston VJ, Oldreive CE, Skowronska A, Oscier DG, Pratt G, Dyer MJ, et al. The PARP inhibitor olaparib induces significant killing of ATM-deficient lymphoid tumor cells in vitro and in vivo. *Blood.* 2010 Nov 25; 116(22):4578–87. doi: [10.1182/blood-2010-01-265769](https://doi.org/10.1182/blood-2010-01-265769) PMID: [20739657](https://pubmed.ncbi.nlm.nih.gov/20739657/)
62. Hong S, Laimins LA. The JAK-STAT transcriptional regulator, STAT-5, activates the ATM DNA damage pathway to induce HPV 31 genome amplification upon epithelial differentiation. *PLoS Pathog.* 2013; 9(4):e1003295. doi: [10.1371/journal.ppat.1003295](https://doi.org/10.1371/journal.ppat.1003295) PMID: [23593005](https://pubmed.ncbi.nlm.nih.gov/23593005/)
63. Shyr C, Tarailo-Graovac M, Gottlieb M, Lee JJ, van Karnebeek C, Wasserman WW. FLAGS, frequently mutated genes in public exomes. *BMC Med Genomics.* 2014; 7:64. doi: [10.1186/s12920-014-0064-y](https://doi.org/10.1186/s12920-014-0064-y) PMID: [25466818](https://pubmed.ncbi.nlm.nih.gov/25466818/)
64. Wang C, Evans JM, Bhagwate AV, Prodduturi N, Sarangi V, Middha M, et al. PatternCNV: a versatile tool for detecting copy number changes from exome sequencing data. *Bioinformatics.* 2014 Sep 15; 30(18):2678–80. doi: [10.1093/bioinformatics/btu363](https://doi.org/10.1093/bioinformatics/btu363) PMID: [24876377](https://pubmed.ncbi.nlm.nih.gov/24876377/)